Mirror-image calibrator for resonant perturbation method in surface resistance measurements of high T_c superconducting thin films

C. K. Ong, Linfeng Chen,[a] Jian Lu, S. Y. Xu, Xuesong Rao, and B. T. G. Tan
Department of Physics, National University of Singapore, Singapore 119260

In surface resistance measurement of high T_c superconducting (HTS) thin films, the conventional resonant perturbation methods have large uncertainties, because their calibrators usually have much larger surface resistance than HTS thin films. This article describes a new type of calibrator, mirror-image calibrator: when the open end of a dielectric resonator is connected to its mirror image, the resonant frequency and quality factor of the resonator are equal to those of the dielectric resonator when its open end is shorted by a perfect conductor. This principle is applied to modify the dielectric resonator method in surface resistance measurement of HTS thin films. The structures of the dielectric resonator for surface resistance measurement (R_s probe) and its mirror-image calibrator are explained in detail. Comparison is made between the present technique and the conventional perturbation technique, and results show that the accuracy and sensitivity of the resonant perturbation method are greatly improved by using the mirror-image calibrator. © *1999 American Institute of Physics.* [S0034-6748(99)03107-X]

I. INTRODUCTION

The microwave surface resistance of superconductors has been an object of intense research since the discovery of superconductivity.[1–3] After the high T_c superconductivity was discovered, high T_c superconducting (HTS) thin films show great application promise in microwave engineering.[4,5] Because the surface resistance of HTS thin films is closely related to the performance of HTS planar microwave devices, many efforts have been made to study the surface resistance of HTS thin films at microwave frequencies, and the methods developed generally fall into two categories: nonresonant methods and resonant methods.

A. Nonresonant methods

Nonresonant methods, including transmission methods and reflection methods, are applicable for the study of vortex dynamics of HTS thin films at microwave frequencies, as the broadband nature of these methods provides a wide ''magnetic field–temperature-frequency'' space.

In a transmission method, the HTS thin film under study forms a quasishort circuit in a waveguide transmission line.[6,7] From the ratio of the transmitted power to the incident power and the phase shift across the HTS thin film, the surface resistance can be deduced. However this method is only suitable for extra thin films whose thickness is less than the penetration depth of the superconductor, and requires a measurement system with very high dynamics range. Because the thicknesses of most of the technologically useful HTS thin films are often larger than the penetration depth, this method is rarely used in the current HTS microwave engineering.

To overcome the attenuation and dynamic range prob-lems of the transmission method, the reflection method is proposed and realized as an alternative to the transmission method. In this configuration, the HTS thin film under study forms a short circuit to a coaxial line, and the complex surface impedance of the HTS thin film can be extracted from the complex reflection coefficient.[8] Because there is electrical current flowing between the inner and the outer conductors of the coaxial line through the HTS thin film, this method requires that both the inner and the outer conductors of the coaxial line have very good electrical contact with the HTS thin film. Booth *et al.*[8] designed a genius structure in the HTS thin film/connector interface by employing a spring-loaded inner conductor pin. However, this method has strict requirements in sample preparation.

B. Resonant methods

The advantage of high accuracy and high sensitivity makes resonant methods widely used in the surface resistance measurement of HTS thin films, although only the surface resistance at one or several discrete frequencies could be measured. The additional advantage that makes resonant methods popular lies in the fact that these methods are nondestructive and so the films after characterization can still be used to fabricate actual devices.

Generally speaking, there are two types of resonators in surface resistance measurement of HTS thin films: hollow metal resonant cavity and dielectric resonator enclosed in a metal shield. Due to the following two distinct advantages, the dielectric resonator method is much more widely used:[9–11] (i) the dielectric resonator method has higher accuracy and sensitivity, and (ii) small samples can be measured at lower frequencies, or different positions in a large sample can be measured.

Usually, a cylindrical dielectric pill located in a cylindrical metal shield is used, and the HTS thin films under study

[a] Author to whom correspondence should be addressed; electronic mail: clinfeng@dso.org.sg
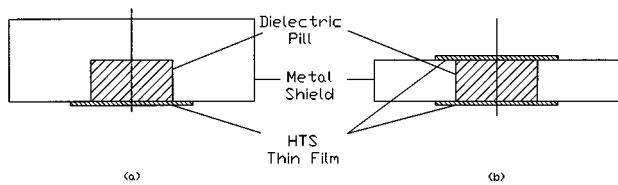
FIG. 1. Dielectric resonators for surface resistance measurement of HTS thin films.

may be placed in contact with one end plane of the pill or with both end planes, as shown in Fig. 1. For the scheme with HTS thin films placed in contact with both end planes of the dielectric pill, as shown in Fig. 1(b), there is an analytic field solution, so the surface resistance can be calculated from the resonant properties of the dielectric resonator.[12–14] However, the disadvantages of this scheme are also obvious: (i) the calculated value of surface resistance is the average value of the two pieces of HTS thin films; and (ii) the calculation ignores the radiation loss, shield loss, and other loss contributions to the quality factor of the dielectric resonator. Fortunately, the above disadvantages could be circumvented, and this scheme has achieved success.

For a scheme with a single piece of HTS thin film placed in contact with one end plane of the dielectric pill, as shown in Fig. 1(a), the surface resistance of the HTS thin film can be measured directly, and with higher sensitivity, although there is no analytical solution for this scheme.[9] Usually, the calibration method, based on resonant perturbation theory, is used to deduce the surface resistance of HTS thin films. However, resonant perturbation theory requires that the surface resistance of the calibrators should be close to those of the HTS thin films under study. As the surface resistance of the best metals (such as silver and gold) is much larger than that of HTS thin films, the surface resistance obtained from the traditional perturbation methods is not very credible.

In this article, a new type of calibrator, the mirror-image calibrator, is employed and so the accuracy and sensitivity of the perturbation method are greatly improved. The structure of the R_s probe and its mirror-image calibrator will be explained in detail. Experimental results show that, because of its sensitivity, accuracy, reliability, simplicity, and nondestructive property, the modified perturbation method is ideal for quality control in the fabrication of HTS thin films.

II. MEASUREMENT PRINCIPLE

A. Resonant perturbation caused by the change of wall loss

According to the resonant perturbation theory,[15,16] the change of the surface impedance ΔZ_s of the film placed in contact with one end of a dielectric resonator causes the change of the formal resonant frequency Δf of the resonator:

$$\Delta f = \frac{i}{2} \Gamma \Delta Z_s,\tag{1}$$

where the real part of Δf corresponds to a shift in the actual resonant frequency f_0 and is associated with the surface reactance of the film, while the imaginary part of Δf corresponds to the change of the reciprocal of the quality factor

$(1/Q)$, and is related to the surface resistance of the film. The resonator constant Γ is determined by the properties of the resonator, and is independent of the sample under study. If we focus our interest on the surface resistance, we have[17]

$$R_{s2} = R_{s1} + A\left(\frac{1}{Q_2} - \frac{1}{Q_1}\right),\tag{2}$$

where R_{s1} is the surface resistance of the original film in contact with the dielectric resonator; R_{s2} is the surface resistance of the sample under study, Q_1 and Q_2 are the quality factors of the dielectric resonator with its end plane in contact with the original film and the sample under study, respectively; and the constant A is only related to the properties of the resonator, and can be determined by calibration.

It should be noted that Eqs. (1) and (2) stand on the assumption that the total stored energy and the field configuration in the resonator do not change due to the introduction of the perturbation.[18] So in Eq. (2), the difference between R_{s1} and R_{s2} should be small. Equation (2) works quite well for the measurement of normal conducting materials, because it is easy to find a calibrator whose surface resistance is close to the surface resistance of the sample under study. However, at microwave frequencies, the surface resistance of high quality HTS thin films is often less than 1 mΩ, while even the surface resistance of the best normal conducting material (such as silver or gold) is at least larger than 10 mΩ. So it is not suitable to deduce the surface resistance of HTS thin films from normal conducting materials using Eq. (2). Besides, if R_{s1} is much larger than R_{s2}, a small uncertainty in the resonator constant A may result in a large error in R_{s2}.

The ideal condition for the measurement of HTS thin film is that the value of R_{s1} in Eq. (2) is zero, which means a zero surface resistance plate. Under this condition, Eq. (2) becomes

$$R_s = A\left(\frac{1}{Q} - \frac{1}{Q_0}\right),\tag{3}$$

where R_s is the surface resistance of HTS thin film under study, and Q_0 and Q are the quality factors of the dielectric resonator when the zero surface resistance plate and the HTS thin film are placed in contact with the dielectric resonator, respectively.

B. Dielectric resonator and its mirror image

In order to increase the accuracy and sensitivity of the resonant perturbation method, a mirror-image calibrator has been employed: when the end plane of the dielectric resonator (R_s probe) is in contact with the mirror image of the probe, the quality factor of the resonator, consisting of the probe and its mirror image, is equal to the quality factor when the end plane of the probe is in contact with an ideal zero surface resistance plate.[19] The principle of the mirror-image calibrator is explained in the following.

The dielectric resonators used for surface resistance measurement of HTS thin films usually are cylindrical dielectric resonators working at the TE$_{011}$ mode. As shown in Fig. 2(a), the TE$_{011}$ mode is axisymmetric, and it has closed
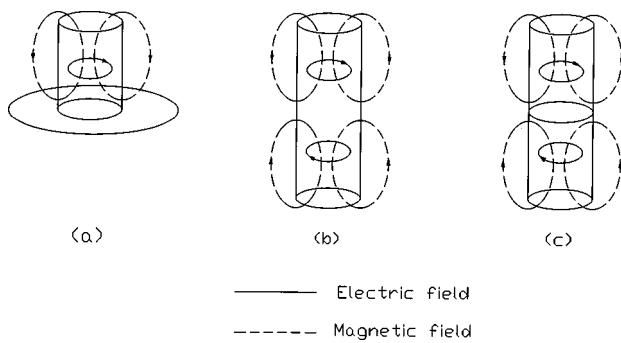
FIG. 2. Field distributions of three dielectric resonators.

FIG. 3. Structures of the R_s probe and its mirror-image calibrator.

loops of transverse electric field, whose centers lie on the axis, and closed loops of magnetic field which lies in planes containing the axis. There is no axial current across any possible joints between the dielectric resonator and the HTS thin film, so this mode is not sensitive to the small gaps between the dielectric resonators and HTS thin films.[12]

Figure 2 shows three cylindrical dielectric resonators, which are made of the same material and have the same diameter d. In Fig. 2(a), the dielectric resonator with length l is in contact with a conducting plate, and it resonates at the TE_{011} mode. The resonator shown in Fig. 2(b) has length $2l$, and resonates at the TE_{012} mode. The resonator shown in Fig. 2(c) also resonates at the TE_{012} mode, and it consists of two pieces of identical dielectric cylindrical pills, each of which has length l. If the surface impedance of the conducting plate shown in Fig. 2(a) is zero, there is no electric field in the plate, and the magnetic field near the plate is parallel to the surface of the plate. From the field distributions of the TE_{011} and TE_{012} modes, we find that the field distribution of the dielectric resonator are shown in Fig. 2(a) is the same as that of the upper part of the dielectric resonator shown in Fig. 2(b), and these two resonators have the same resonant frequency. As the plate shown in Fig. 2(a) does not dissipate microwave energy, the dielectric resonator shown in Fig. 2(b) has twice the stored energy, and at the same time twice the energy dissipation as the dielectric resonator shown in Fig. 2(a). Therefore, they have the same quality factor.[20] Because there is no axial current across the plane perpendicular to the axis at the middle of the cylinder, a small gap perpendicular to the axis at the middle of the cylinder hardly affects the resonant properties of the resonator. As such, the resonator shown in Fig. 2(a) and the one shown in Fig. 2(c) also have the same resonant frequency and quality factor. In our experiments, the size of the gap between the two pieces of dielectric pills is close to the light wavelength that is much smaller than the microwave wavelength, so the uncertainty caused by the gap is negligible.

The above discussions show that, if the zero surface resistance plate shown in Fig. 2(a) is replaced by the mirror image of the dielectric resonator, although the electromagnetic boundary condition of the dielectric resonator is changed from a short circuit condition to an open-circuit condition, its quality factor does not change. Therefore, the quality factor of the dielectric resonator, when it is connected to its mirror-image structure, can be used as Q_0 in Eq. (3). In
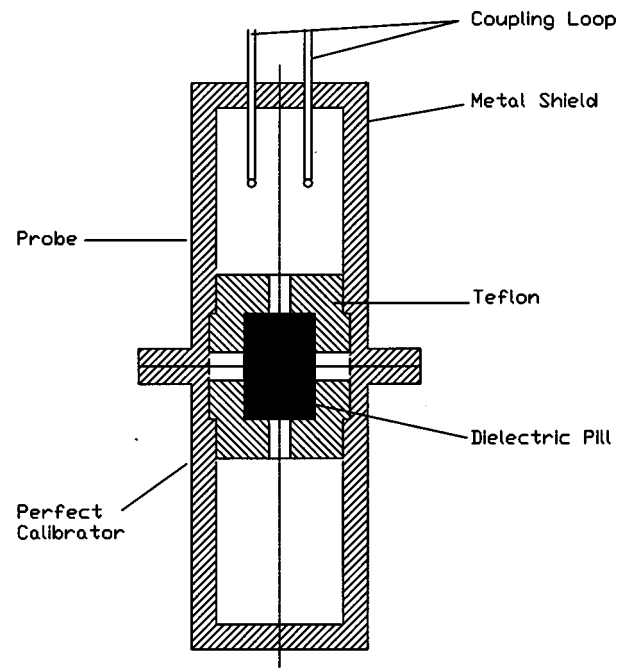
this article, the mirror-image structure is also called the mirror-image calibrator.

III. EXPERIMENTS

A. R_s probe and its mirror-image calibrator

In our experiments, the R_s probe is a TE_{011} cylindrical dielectric resonator, and its working frequency is 10.65 GHz. Its mirror-image calibrator is a dielectric pill that is made of the same material and has the same dimensions as the R_s probe. Figure 3 shows our R_s probe at a calibration state: the probe (the upper part) is in contact with its mirror-image calibrator (the lower part). The probe and its mirror-image calibrator have the same structures except that the probe has two coupling loops, while the mirror-image calibrator does not have. The key components of the probe and the mirror-image calibrator are the dielectric pills, the Teflon holders, and the metal shields.

1. Dielectric pills

The probe and its mirror-image calibrator have the same dielectric pills. Each dielectric pill is a piece of $LaAlO_3$ single crystal with dimensions: $\Phi6.0 \times 5.5$ in mm, and the two dielectric pills are made from the same piece of $LaAlO_3$ single crystal, and the symmetrical axis of each dielectric pill is the c axis of the crystal. The two end planes of each dielectric pill are finely polished. When the two dielectric pills are connected by end plane to end plane, as shown in Figs. 2(c) and 3, light interference fringes can be observed, indicating that the size of the gap between the two dielectric pills is on the order of light wavelength. Besides, experiments made at room temperature show that the two TE_{011} mode dielectric resonators (formed by sandwiching each of the two dielectric pills between two conducting plates) and the TE_{012} mode resonator (formed by sandwiching two di-
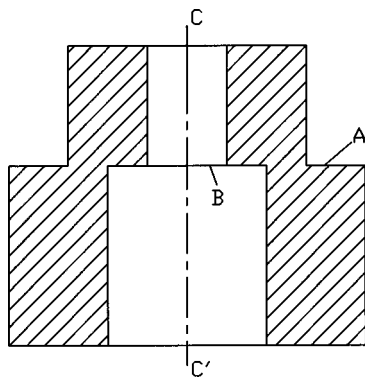
FIG. 4. Structure of the Teflon holder.

TABLE I. Calibrations of Eqs. (2) and (3). Equation (3) is calibrated twice, as indicated by calibration (I) and calibration (II). All the calibrations are performed at 10.65 GHz and 77 K.

	Calibration of Eq. (2)	Calibration (I) of Eq. (3)	Calibration (II) of Eq. (3)
Mirror-image calibrator	⋯	$Q_0 = 31\,095$	$Q_0 = 31\,095$
Silver plate	$R_{s1} = 11.5$ mΩ $Q_1 = 15\,126$	$R_s = 11.5$ mΩ $Q = 15\,126$	⋯
Gold plate	$R_{s2} = 20.8$ mΩ $Q_2 = 10\,879$	⋯	$R_s = 20.8$ mΩ $Q = 10\,879$
A	3.603×10^5	3.387×10^5	3.481×10^5

electric pills connected face to face between two conducting plates) have the same resonant frequency and quality factor.

2. Teflon holders

The structures of the Teflon holders in the probe and the mirror-image calibrator are shown in Fig. 4. The relative position between the $LaAlO_3$ single crystal and the metal shield should not change when the temperature changes from room temperature to liquid nitrogen temperature. Because the thermal expansion coefficient of Teflon is much larger than those of brass and $LaAlO_3$, special attention has been paid to the design of the Teflon holders: (i) planes A and B are in the same plane perpendicular to the c-c' axis, so the perpendicular distance between these two planes is always zero at any temperature; (ii) the tolerances of the Teflon holder are carefully selected to ensure the Teflon holder can tightly hold the $LaAlO_3$ pill at any temperature; (iii) the hole in the top of the holder is used to observe whether the dielectric pill is correctly assembled; and (iv) there is a groove (not shown in Fig. 4) to release the gas pressure difference between the upper and lower part of the probe.

It should be noted that Teflon is lossy material compared to $LaAlO_3$ single crystal. The Teflon holders add losses to the probe and its mirror-image calibrator, and thus lower the value of Q_0. If lower-loss materials with good mechanical and thermal properties are available, the measurement resolution of the probe could be further increased.

3. Metal shield

The metal shields do not resonate at the working frequency of the dielectric resonators, prohibiting the microwave radiation from the dielectric resonators. In order to decrease their wall loss contributions to the quality factors of the dielectric resonators, the brass shields are coated with silver. Besides, the shields are sealed with indium wire and the samples are separated from the liquid nitrogen, and can be kept in special gas environments that we prefer. In our following experiments, the R_s probe is sealed in a helium environment.

B. Calibration

Equations (2) and (3) are often used for the measurement of the surface resistance of conducting plates. For the mea-

surement of HTS thin films, Eq. (3) is more accurate and sensitive provided that the mirror-image calibrator corresponding to the probe is available. Whichever equation is used, calibration is needed to determine the resonant constant A. In order to make a comparison between the present technique and the conventional perturbation technique, we calibrated both Eqs. (2) and (3).

In our calibration procedure, three calibrators are used: the mirror-image calibrator discussed above and two conventional calibrators. One of the two conventional calibrators is a silver plate whose surface resistance is 11.5 mΩ, and the other is a gold plate whose surface resistance is 20.8 mΩ. The calibration results are shown in Table I. In Table I, the silver plate and the gold plate are used to calibrate Eq. (2). Equation (3) is calibrated twice by the silver plate and the gold plate separately and independently, to check whether the selection of the conventional calibrator is crucial in the present technique.

It should be pointed out that, before every set of measurements, fresh calibration is required, because the properties of the probe may change due to the change of environment, such as temperature, moisture, etc.

C. Uncertainty analysis

The uncertainties of the present technique mainly consist of two parts: the calibration uncertainty and measurement uncertainty. In our experiments, the microwave measurements are performed on the HP 8722D vector network analyzer, and we find that the measurement uncertainty is much smaller than the calibration uncertainty.

The calibration uncertainty is mainly related to two factors: the quality of the mirror-image calibrator and the repeatability of the mechanical assembly. The quality of the mirror-image calibrator is determined by the extent to which the probe and the mirror-image calibrator are identical. To minimize the uncertainty, the two dielectric pills, the two metal shields, and the two Teflon holders in the probe and the mirror-image calibrator are made as similar as possible. The only difference between the probe and the mirror-image calibrator is that there are two coupling loops in the probe, while there is no coupling loop in the mirror-image calibrator. However the uncertainty caused by such a difference is negligible because the couplings are very weak. So the calibration uncertainty is mainly determined by the uncertainty of the mechanical assembly.

TABLE II. Different results of surface resistance measurements following different calibrations. The samples are YBCO thin films fabricated on LaAlO$_3$ substrates. All the measurements are made at 10.65 GHz and 77 K.

Item numbers of HTS thin films	Q_2 in Eq. (2) or Q in Eq. (3)	R_s values following Eq. (2)	R_s values following Eq. (3) with calibration (I)	R_s values following Eq. (3) with calibration (II)
1	21 379	4.533 1	4.950 2	5.087 6
2	24 835	2.187 8	2.745 6	2.821 8
3	27 104	0.973 3	1.603 9	1.648 4
4	28 752	0.211 29	0.887 62	0.912 26
5	29 563	−0.132 38	0.564 46	0.580 13
6	29 861	−0.254 01	0.450 13	0.462 62

In our experiments, the calibration uncertainty is about 150 $\mu\Omega$, and the measurement uncertainty is about 10 $\mu\Omega$. So the absolute uncertainty of the surface resistance is about 160 $\mu\Omega$, and the surface resistance values are in 10 $\mu\Omega$ resolution.

Of course, the uncertainty of the present technique could be further reduced if (i) dielectric pills with higher Q value are available; (ii) holders with lower loss are available; (iii) better structure of the probe and its mirror-image calibrator could be designed; and (iv) higher mechanical fabrication precision could be achieved.

IV. RESULTS AND DISCUSSION

To make a comparison between the conventional perturbation method and the modified perturbation method, we measured the surface resistance of YBCO thin films using the conventional dielectric resonator technique and the technique presented in this article. The YBCO thin films are fabricated on LaAlO$_3$ substrates by using pulsed laser ablation techniques,[21] and their thickness is around 5000 Å. Our measurement results are shown in Table II.

In Table II, the surface resistance of each piece of YBCO thin film is calculated in three different ways according to the three calibrations we have made. To make a detailed comparison of the calculation results according to different calibrations, we list five decimal digits for each R_s value. Table II shows that the results following two calibrations of Eq. (3) are obviously more accurate and credible than the ones following Eq. (2). The differences in the calculation results caused by the different calibrators in calibrations (I) and (II) of Eq. (3) are acceptable. So in the present technique, the selection of the conventional calibrator is not

very crucial, and even if there is some error in the surface resistance value of the conventional calibrator, the effect caused by such error is not very severe. For the conventional technique, Eq. (2) could give understandable results for the HTS thin films with large surface resistance (items 1–3). However, for HTS thin films with low surface resistance, the results following Eq. (2) are unbelievable (items 5 and 6). Besides, if there is any uncertainty in the surface resistance values of the two conventional calibrators, the results following Eq. (2) will have much larger uncertainties.

Finally, it should be noted that the mirror-image calibrator presented in this article is an equivalent zero-impedance structure, so its equivalent reactance is also zero. The modification presented in this article may be extended to study the surface reactance of HTS thin films.

[1] J. R. Waldram, Adv. Phys. **13**, 1 (1964).

[2] A. M. Portis, *Electromagnetics of High-Temperature Superconductor* (World Scientific, Singapore, 1993).

[3] M. Tinkham, *Introduction to Superconductivity*, 2nd ed. (McGraw–Hill, New York, 1996).

[4] M. J. Lancaster, *Passive Microwave Device Applications of High-Temperature Superconductors* (Cambridge University Press, Cambridge, 1997).

[5] Z. Y. Shen, *High-Temperature Superconducting Microwave Circuits* (Artech House, Boston, 1994).

[6] D. Dew-Hughes, in *Microwave Physics and Techniques*, edited by H. Groll and I. Nedkov (Kluwer Academic, Dordrecht, 1997), pp. 83–114.

[7] R. X. Wu and M. Qian, Rev. Sci. Instrum. **68**, 155 (1997).

[8] J. C. Booth, D. H. Wu, and S. M. Anlage, Rev. Sci. Instrum. **65**, 2082 (1994).

[9] C. J. Edgcombe and J. R. Waldram, *Research Review 94, IRC in Superconductivity* (University of Cambridge Press, Cambridge, 1994), p. 50.

[10] S. J. Fiedziusko and P. D. Heidmann, IEEE MTT-S Digest 555 (1989).

[11] J. Gallop, L. Hao, and F. Abbas, Physica C **282–287**, 1579 (1997).

[12] Y. Kobayashi and M. Katoh, IEEE Trans. Microwave Theory Tech. **33**, 586 (1985).

[13] Z. Y. Shen, C. Wilker, P. Pang, W. L. Holstein, D. Face, and D. J. Kountz, IEEE Trans. Microwave Theory Tech. **40**, 2424 (1992).

[14] W. L. Holstein, L. A. Parisi, Z. Y. Shen, C. Wilker, M. S. Brenner, and J. S. Martens, J. Supercond. **6**, 191 (1993).

[15] L. D. Landau and E. M. Lifshitz, *Electrodynamics of Continuous Media* (Pergamon, New York, 1960).

[16] R. J. Ormeno, D. C. Morgen, D. M. Broun, S. F. Lee, and J. R. Waldram, Rev. Sci. Instrum. **68**, 2121 (1997).

[17] D. N. Kourov and A. S. Shcherbakov, Rev. Sci. Instrum. **67**, 274 (1996).

[18] L. F. Chen, C. K. Ong, and B. T. G. Tan, Meas. Sci. Technol. **7**, 1255 (1996).

[19] J. Lu, X. Y. Ren, and Q. S. Zhang, *ICCS '94* (IEEE, Singapore, 1994), p. 959.

[20] Y. Kobayashi and S. Tanaka, IEEE Trans. Microwave Theory Tech. **28**, 1077 (1980).

[21] B. L. Low, S. Y. Xu, C. K. Ong, X. B. Wang, and Z. X. Shen, Supercond. Sci. Technol. **10**, 41 (1997).